Flexural-Torsional Buckling and Its Implications for Steel Compression Member Design

CYNTHIA J. ZAHN and NESTOR R. IWANKIW

INTRODUCTION

Flexural-torsional and torsional buckling strength of compression members is covered for the first time in the AISC Load and Resistance Factor Design (LRFD) Specification,[1] and, thus, must now be considered in hot-rolled steel design for buildings, in addition to overall flexural and local buckling (Fig. 1). This new strength criterion is also included in the 1989 Allowable Stress Design (ASD) Specification.[13] As illustrated in Fig. 1, flexural-torsional buckling is a compression member instability involving a combination of member bending and twisting as well as any local buckling of slender elements. In this behavioral sense, it resembles lateral-torsional buckling of unbraced beams. Torsional buckling is simply a twisting of the entire cross section about its shear center. Flexural-torsional buckling applies to all shapes except those that are doubly symmetric. Pure torsional buckling can only occur in these doubly symmetric shapes, such as rolled wide flange sections.

Flexural-torsional buckling is strongly influenced by the degree of symmetry in a cross section that is mathematically represented by the location of the shear center relative to the centroid. An interactive coupling effect of flexural and torsional buckling occurs only when these two points are not coincident; when they are identical, as for doubly symmetric, wide-flange shapes, the response reduces to pure torsional buckling.

Generally, for hot-rolled columns, truss and bracing compression members, which are usually relatively stocky with at least one axis of symmetry, and with effective lengths KL of about 10 ft or more, these new limit states either do not govern or the reduced critical load differs insignificantly from the weak-axis flexural buckling load. Furthermore, closed symmetric cross sections, such as pipes and tubes, are torsionally very strong and their capacity will ordinarily not be limited by torsional buckling. Flexural-torsional or torsional buckling more often controls the design capacity of shorter built-up compression members made from thin plate elements with unsymmetric open cross sections or rolled single angles. For this reason, AISI cold-formed steel design specifications[2] have for many years included flexural-torsional buckling criteria, based on theory that has been well documented for several decades in many references and advanced texts. The LRFD and ASD Specifications now also require that a check of these limit states be made.

Many structural engineers are probably somewhat unfamiliar with flexural-torsional buckling theory and its meaning, as the authors initially were prior to a study of the existing literature and several sample calculations. Hence, this article will attempt to provide some useful overview and practical understanding of this strength limit state. Numerical comparisons have been made to identify general trends, sensitivity to key design variables, and conclusions. Refs. 3 and 4 cover similar material pertaining exclusively to double angles.

FLEXURAL-TORSIONAL BUCKLING PROVISIONS IN LRFD

According to LRFD Specification Appendix E3,* the compressive design strength based on the limit states of torsional and flexural-torsional buckling is $\phi_c P_n$, where ϕ_c is 0.85 and

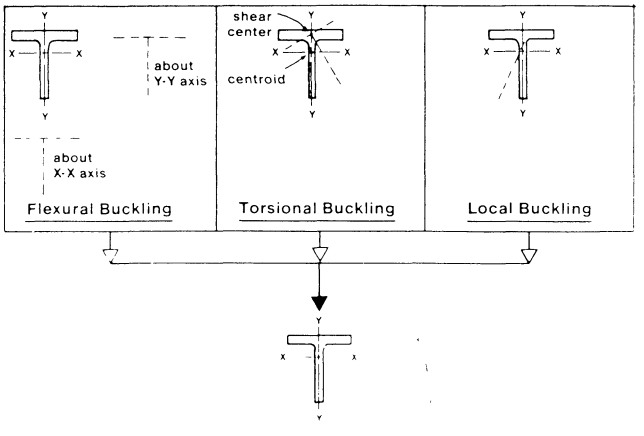

Fig. 1. Flexural-torsional buckling

Cynthia J. Zahn is staff engineer–Structures, AISC, Chicago.

Nestor R. Iwankiw is director, Research and Codes, AISC, Chicago.

**All references to formulas, Appendices, and Sections are to the LRFD Specification, which covers flexural-torsional buckling in detail.*

P_n is the product of A_g and F_{cr}. The critical stress F_{cr} is determined from the general column design curves representing the inelastic and elastic flexural buckling zones, including reduction factors Q and λ_e:

$$\text{For } \lambda_e \sqrt{Q} \leq 1.5 \text{ (inelastic)}$$
$$F_{cr} = Q(0.658^{Q\lambda_e^2})F_y \qquad \text{(A-E3-2)}$$

$$\text{For } \lambda_e \sqrt{Q} > 1.5 \text{ (elastic)}$$
$$F_{cr} = \left[\frac{0.877}{\lambda_e^2}\right]F_y \qquad \text{(A-E3-3)}$$

The local buckling reduction factor Q is dependent on the compression element slenderness and boundary conditions and it is defined identically to the 8th Edition Allowable Stress Design (ASD) Specification.[5] However, Q does not include the additional reduction in overall flexural-torsional coupling effects for singly symmetric and unsymmetric shapes. Thus, in order to fully account for this latter effect, the new equivalent column slenderness λ_e from LRFD Appendix E must be evaluated. The flexural-torsional buckling equations are based on elastic buckling theory of an idealized column, i.e., perfectly straight member with no residual stresses. As the member slenderness approaches zero, all elastic buckling stresses tend toward infinity. The adjusted slenderness λ_e converts those theoretical equations for use in "real" column design (the general column design F_{cr} curves), thereby automatically including residual stress, out of straightness, and yielding effects with a maximum F_{cr} equal to the yield stress, where

$$\lambda_e = \sqrt{\frac{F_y}{F_e}} \qquad \text{(A-E3-4)}$$

There are three different Appendix E equations for F_e, the critical elastic buckling stress, depending on the design of column section symmetry.

For unsymmetric shapes (i.e., unequal leg single angles), flexural buckling about the two principal axes, X–X and Y–Y, interacts with pure torsional buckling to produce the most complex flexural-torsional buckling solution. This is due to the shear center being offset from the centroid in both the X and Y principal directions (see Fig. 2). Note that the AISC Manual Part 1 coordinate system designates X and Y as the horizontal and vertical geometric axes and Z as the minor principal axis, whereas X and Y in the context of this article refer to the principal axes, and Z to the longitudinal torsional axis along the shear center. For this unsymmetric case, the critical elastic buckling stress is the lowest of the three possible roots of the cubic equation,[6,7,8]

$$(F_e - F_{ex})(F_e - F_{ey})(F_e - F_{ez}) - F_e^2(F_e - F_{ey})(x_o/\bar{r}_o)^2 - F_e^2(F_e - F_{ex})(y_o/\bar{r}_o)^2 = 0 \qquad \text{(A-E3-7)}$$

The lowest root F_e or the stress at which the member will theoretically become elastically unstable is always less than either of the Euler flexural buckling stresses, F_{ex} and F_{ey}, and F_{ez}, the pure torsional buckling stress about the shear center, which are defined as

$$F_{ex} = \frac{\pi^2 E}{(K_x l/r_x)^2} \qquad \text{(A-E3-10)}$$

$$F_{ey} = \frac{\pi^2 E}{(K_y l/r_y)^2} \qquad \text{(A-E3-11)}$$

$$F_{ez} = \left[\frac{\pi^2 E C_w}{(K_z L)^2} + GJ\right]\frac{1}{A\bar{r}_o^2} \qquad \text{(A-E3-12)}$$

The flexural-torsional properties C_w, J, and $\bar{r}_o$, are all tabulated in Part 1 of the LRFD Manual of Steel Construction.[1] The polar radius of gyration about the shear center $\bar{r}_o$ is defined by one formula for all shapes:

$$\bar{r}_o^2 = x_o^2 + y_o^2 + \frac{I_x + I_y}{A} \qquad \text{(A-E3-8)}$$

The above expression is easily derived from the polar moment of inertia about the centroid $(I_x + I_y)$ by use of the parallel axis theorem. For doubly symmetric shapes (wide flanges), $x_o = y_o = 0$ and $A\bar{r}_o^2$ reduces to simply $(I_x + I_y)$. Similar to lateral-torsional buckling of beams, torsional buckling strength of columns consists of both warping and St. Venant (pure torsion) components, which correspond to the first and second terms in the parentheses of Eq. A-E3-12, respectively. The warping constant C_w and torsional constant J vary for the different shapes and their exact formulas can be found in textbooks, such as Bleich[9] or Reference 10. The conventional approximation for J in open sections com-

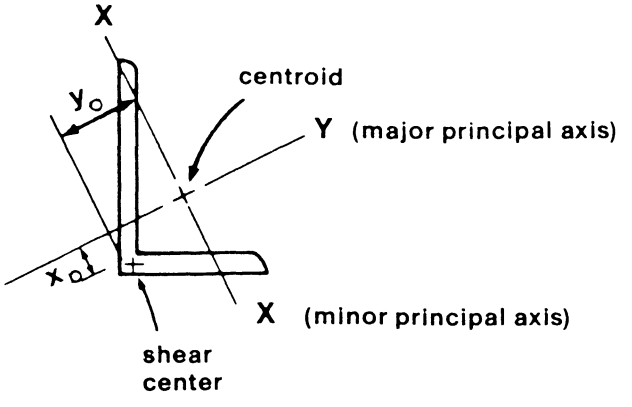

Fig. 2. Unsymmetric single angle

posed of thin plate elements of length b and thickness t is $J = (1/3)\Sigma bt^3$, while

$$C_w \approx \frac{d^2 I_c I_t}{I_c + I_t}$$

for singly symmetric I-shapes, I_c and I_t being the moments of inertia for the compression and tension flanges, respectively.

The flexural-torsional elastic buckling stress for singly symmetric shapes (i.e., double angles, equal leg single angles, WTs, channels), where Y is the axis of symmetry (see Fig. 3) is:

$$F_e = \frac{F_{ey} + F_{ez}}{2H}\left[1 - \sqrt{1 - \frac{4F_{ey}F_{ez}H}{(F_{ey} + F_{ez})^2}}\right] \quad \text{(A-E3-6)}$$

where H = flexural constant = $1 - \left(\frac{x_o^2 + y_o^2}{\bar{r}_o^2}\right)$

H is a section property, also tabulated in the LRFD Manual for angles, tees, and channels, which represents the degree of symmetry in the cross section. It is not defined for unsymmetric sections and reaches its upper bound of 1.0 for doubly symmetric shapes. This singly symmetric F_e solution is derived from the previous unsymmetrical general case with $x_o = 0$, since the shear center is on the principal Y-axis. As this formula indicates, for singly symmetric shapes flexural-torsional buckling occurs when Y-Y axis flexural buckling and torsional buckling interact. As shown in Fig. 4, F_e is again always less than either F_{ey} or F_{ez}, the variables in Eq. A-E3-6, but it may be greater or less than F_{ex} depending on whether X is the major or minor axis. Therefore, a singly symmetric shape will buckle in one of two modes, flexural-torsional or simple X–X flexural buckling, where the X–X axis elastic buckling strength is defined by Eq. A-E3-10, as stated earlier.

For doubly symmetric sections (i.e., I-shapes, cruciforms) the shear center and centroid always coincide, therefore $x_o = y_o = 0$ and $H = 1.0$, and consequently Eq. A-E3-7 simplifies to

$$(F_e - F_{ex})(F_e - F_{ey})(F_e - F_{ez}) = 0$$

There are three possible independent roots to this equation, F_{ex}, F_{ey}, and F_{ez}. Since no interaction occurs between the torsional term F_{ez} and either of the flexural terms, F_{ex} and F_{ey}, F_e for a doubly symmetric shape is the lower of F_{ex}, F_{ey}, or F_{ez}, as defined in Eqs. A-E3-10 through A-E3-12. Equation A-E3-6 similarly defaults to $F_e = F_{ey}$ or F_{ez} for $H = 1.0$.

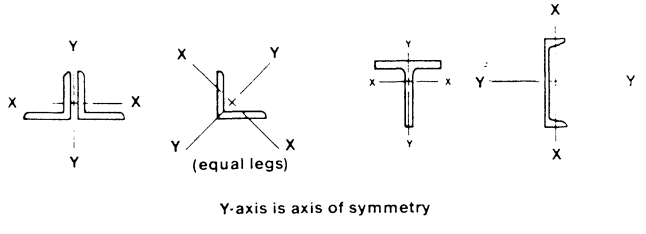

Fig. 3. Singly symmetric shapes

FLEXURAL-TORSIONAL BUCKLING IN ASD

Flexural-torsional buckling for compression members is briefly covered in the updated 1989 ASD Specification (Sect. E3) and included in the design aids for the new 9th Edition AISC Manual. The main conversion formula for equivalent member slenderness is given in the ASD Commentary:

$$\frac{Kl}{r_e} = \pi\sqrt{\frac{E}{F_e}}$$

wherein F_e is the elastic buckling stress, as defined in LRFD.

IMPACT OF NEW PROVISIONS

This paper addresses only the behavior and design of centrally loaded compression members. Any applied bending moments and end restraint effects must be evaluated, as usual, in conjunction with the beam-column interaction formula and the effective length factor K. Any effects of compression load eccentricity relative to the centroid should also be checked.

The effect of the new flexural-torsional or torsional buckling criteria on the strength of a centrally loaded column design depends on the member's geometry and the thickness of its components. In general, these limit states are most important for columns with unsymmetric open cross sections and slender elements. These types of members are not among the standard hot-rolled structural steel shapes, except for un-

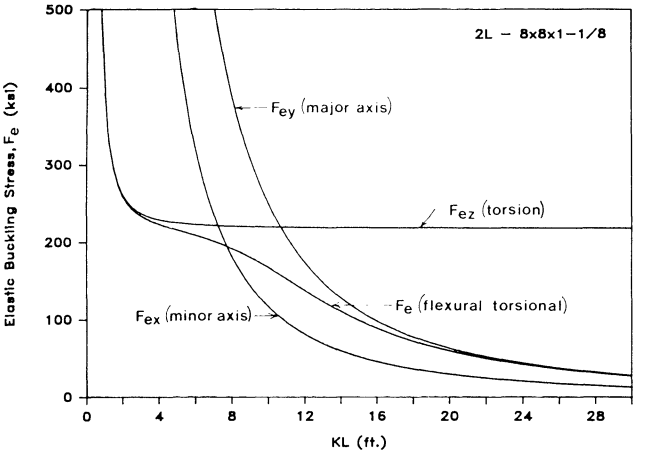

Fig. 4. Elastic buckling curves for a singly symmetric shape

equal leg single angles, and will not be addressed further here. A separate and new 1989 AISC Specification on single angle design has been developed to satisfy this particular need.[13,14] Most of the ensuing discussion will focus on flexural-torsional buckling strength of the more common singly symmetric shapes. In addition, pure torsional buckling effects on doubly symmetric shapes will be summarized.

Singly Symmetric Shapes

The effect of flexural-torsional buckling on singly symmetric member strength was found to primarily depend on cross section geometry, member slenderness, and bracing locations. The relative importance of the warping constant C_w on the overall flexural-torsional buckling curve was also analyzed.

Several plots of nominal critical stress F_{cr} versus effective length KL were made for selected WTs, double angles, channels, and equal leg single angles, all for A36 steel. The critical stress F_{cr} based on the LRFD column design curve was calculated for X–X, Y-Y, and flexural-torsional (F–T) buckling. In all cases, flexural-torsional buckling reductions were greatest for the lower KL values, about 10 ft and less. As shown in Figs. 5 and 6, this limit state may or may not control for larger KL values. Flexural-torsional buckling marginally governs for the entire range of KL values for the heavier WT18×179.5 (Fig. 5), with the maximum difference being less than 10% at a KL of approximately 5 ft. For the WT4×12 (Fig. 6), the F–T curve crosses over the minor X–X axis curve when KL is approximately 4 ft.

Consistent with the observations in Ref. 8, the corresponding plots for other singly symmetric shapes demonstrate that if the axis of symmetry, Y-Y, is also the minor principal axis, flexural-torsional buckling controls the strength for all KL values, but the difference from the minor axis flexural buckling strength at larger unbraced lengths is usually negligible for design purposes. On the other hand, if the Y-Y axis is the major principal axis as it is for equal leg single angles and channels, F–T buckling governs only for smaller KL values or not at all, while minor X–X flexural buckling governs for the other unbraced lengths. For equal leg single angles and channels, the latter case is always true. On the other hand, double angles situated long legs back to back (LLBB) and short legs back to back (SLBB) illustrate both situations. In Fig. 7, F_{cr} versus KL is plotted for double angles 8×4×1 (LLBB) where the Y-Y axis is the weak axis and F–T buckling always governs with the curve falling just below the Y-Y buckling curve. The maximum effect occurs at KL = 2.25 ft wherein the F–T F_{cr} curve is about 4.7% lower than the Y-Y axis critical stress curve. This difference decreases relatively quickly and, beyond KL = 9.5 ft, there is negligible difference of less than 3% between the two curves. Conversely, Fig. 8 is the graph of double angles 8×4×1 (SLBB), where the Y-Y axis is the strong axis and F–T buckling governs only for very small KL values.

Based on sample analyses, member slenderness KL is of secondary importance to section geometry for flexural-torsional buckling. More slender section elements could increase the reduction by a substantial amount in some cases. Two illustrative examples are given here: one wherein the Y-axis of symmetry is the weak axis and another where it is the strong axis. Considering the first case, Figs. 9a and 9b give F_{cr} plots for a WT15×105.5 and a WT18×179.5, respectively. Although the shapes of the buckling curves are similar, F–T buckling is slightly more significant for the more slender WT15×105.5 with a stem thickness of 0.775 in. and flange thickness of 1.315 in. than for the stockier WT18×179.5 with a stem thickness of 1.12 in. and flange thickness of 2.01 in. Figure 10 is a graph of percent difference between the F–T and Y-Y minor axis buckling curves for both shapes. The maximum percent difference occurs near KL = 4 ft in

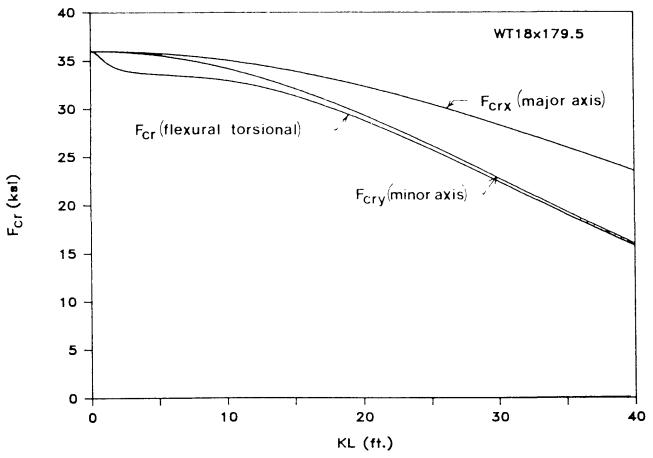

Fig. 5. Critical stress for WT18 × 179.5

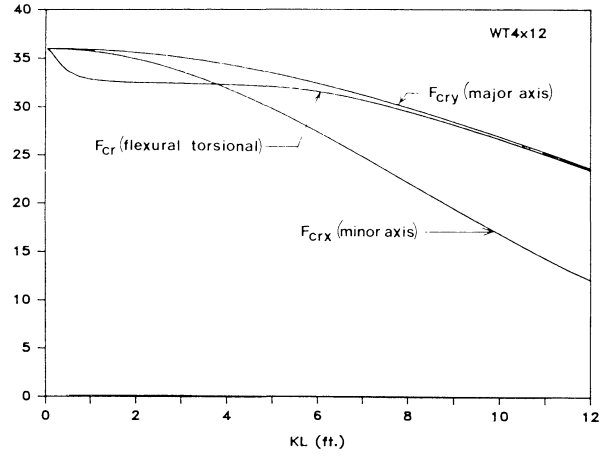

Fig. 6. Critical stress for WT4 × 12

both cases; however, the maximum is approximately 10.7% for the more slender shape versus 6% for the WT18×179.5. Although the maximum F-T effects for both shapes occur at low effective lengths, the percent F_{cr} reduction relative to minor axis flexural buckling exceeds a given percentage for a wider range of effective lengths in the thinner shape.

Local slenderness has a similar effect on the strength of columns when the strong axis is the axis of symmetry. Figures 11a and 11b give graphs of F_{cr} versus KL for an L8×8×1⅛ and an L8×8×¾, where F-T buckling governs only at small KL values. The 1⅛ in. thick angle's F-T curve crosses the X-X curve at approximately 4.5 ft, while this intersection occurs at KL slightly greater than 10 ft for the thinner ¾ in. angle. For a thinner angle, flexural-torsional buckling becomes critical for a wider range of KL values as the entire buckling curve is lower in comparison. Since the minimum radius of gyration r_x for both angles is about 1.60, the reduction in the F-T buckling curve in these two cases can be attributed to the torsional term F_{ez}, as defined in Eq. A-E3-12. The main section properties affecting F_{ez} are the warping constant C_w and the torsional constant J. As will be discussed subsequently, any effect of EC_w is limited to much shorter KL values. Therefore, the lowered F_{cr} F-T curve must be due to the reduced torsional rigidity, and thus GJ, associated with thinner members.

Values of C_w for WTs and angles are small compared to I-shapes.[1] A good measure of the relative warping to pure torsional stiffness of a given section is

$$a = \sqrt{\frac{EC_w}{GJ}}$$

The smallest such ratio for rolled I-shapes is approximately 20. For larger WTs and angles, a may reach 4 or 5, or only about 25% of the weakest I-shape warping strength. In Fig. 12, for a WT18×179.5, F_{cr} versus KL is plotted for X-X axis buckling, Y-Y axis buckling, and flexural-torsional buckling with and without C_w. With the larger C_w value of 480 in.[6] and a equal to 4.7, this shape gives a good indication of the maximum beneficial effect the inclusion of warping would have on the F-T buckling curve for WT and singly symmetric angle shapes at lower unbraced lengths. It is apparent from this plot and the similarity of the warping term in F_{ez} to the Euler flexural buckling formula that the warping effect quickly diminishes with increasing KL values. In this case, including C_w allows a slightly higher nominal strength only for KL values less than approximately 10 ft. Therefore, some strength advantage can be gained by including C_w if short unbraced lengths are involved. This strength advantage is applicable to a wider range of lengths for channels as show in Fig. 13 for a C15×33.9.

Channels have slightly greater a values in general, resulting in a greater decrease in strength with $C_w = 0$ before the two flexural-torsional curves coincide. However, it is easier and always conservative to ignore C_w for WTs, double and single angles, as often has been done by many authors in the literature, thereby simplifying Eq. A-E3-12 to

$$F_{ez} = (GJ)\frac{1}{A\bar{r}_o^2}$$

which is a constant independent of KL. However, the AISC LRFD Manual[1] has included C_w contributions in the design capacity of these members.

Finally, different unbraced lengths in the X and Y directions and for flexural-torsional buckling must be considered. Flexural-torsional buckling may control the column strength if sufficient bracing is not provided, even if the F-T curve falls above the X or Y buckling curves.

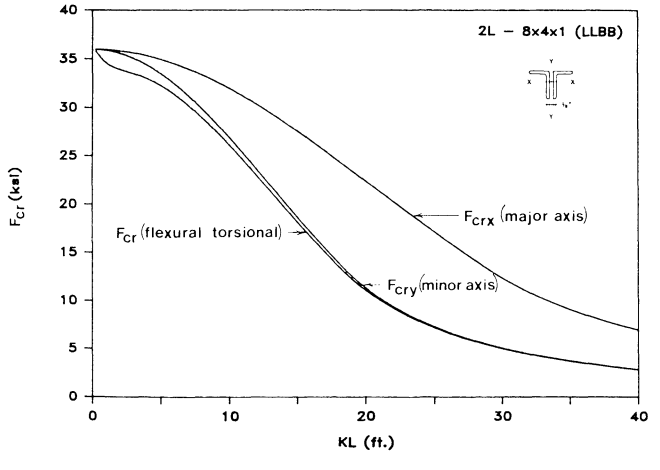

Fig. 7. Critical stress for double angles, long legs back-to-back (LLBB)

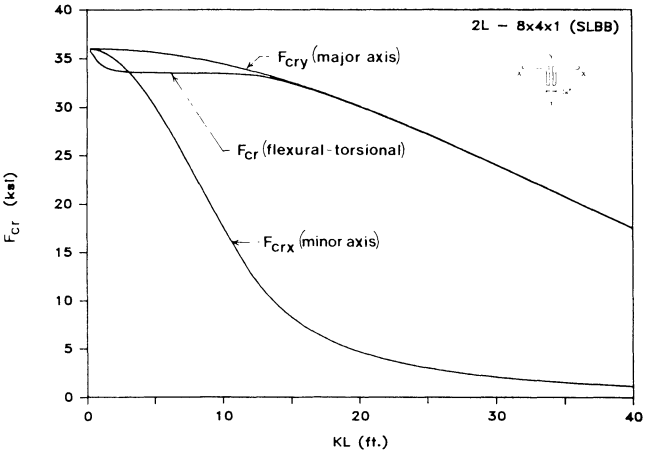

Fig. 8. Critical stress for double angles, short legs back-to-back (SLBB)

Doubly Symmetric Shapes

As discussed earlier, since the shear center location is identical to the centroid of a doubly symmetric shape, flexural and torsional buckling do not interact. The applicable limit states are the separate X–X and Y–Y flexural buckling and Z–Z torsional buckling limit-states. For most compact I-shapes, torsional buckling can be simply ignored with the weak Y-axis buckling controlling the strength. The influential variables are the flange width to section depth ratio (b_f/d), the warping constant C_w and the maximum unbraced length against twist.

Torsional buckling has been found to be important only for those I-shapes with rather short lengths and wider flanges.[10] This is evidenced by comparing Figs. 14 and 15; plots of F_{cr} versus KL for a F_y = 36 ksi, W10×22 and W12×65 respectively. For the W10×22, with a lower flange width to member depth ratio of 0.57, the Y-Y buckling curve is always the lowest. The (b_f/d) = 0.99 ratio is considerably higher for the W12×65, and the torsional buckling curve drops slightly below the Y-Y curve until KL reaches 7 ft. This graph is representative of W shapes with higher (b_f/d) ratios. Even in this case, the maximum difference between the two curves is much less than 1%, an inconsequential deviation for design purposes.

The general insignificance of torsional buckling on the strength of W shapes can be attributed to its sensitivity to the previously defined ratio a. The relatively large EC_w value for W-shapes raises the torsional buckling curve such that it does not govern their strength. This is demonstrated in both Figs. 16 (an extension of Fig. 15) and 17, where plots for a 36 ksi W12×65 and W12×336 are given for X–X, Y-Y, and torsional buckling. The torsional buckling curve is also given with C_w = 0. It is evident from these curves that torsional buckling would govern only in the lower KL range if C_w were ignored; the amount of which is dependent on the a ratio. For the W12×65, a = 82.9 and for the W12×336, a = 24.7. As expected, the larger a value for the lighter W-shape indicates that EC_w is more dominant than GJ and vice versa for the smaller a value. The GJ component for the W12×65 in Fig. 16 is found to be only 64% of the total and torsional buckling based on GJ alone governs for KL values up to approximately 25 ft. These are typical effective lengths for design and, therefore, C_w is very important in this case. For the W12×336 in Fig. 17, however, the GJ contribution is 97% of the full torsional buckling strength. Also, torsional buckling based on GJ alone governs only to KL = 7 ft. For these reasons, it would be feasible to conservatively ignore the EC_w term in the torsional buckling

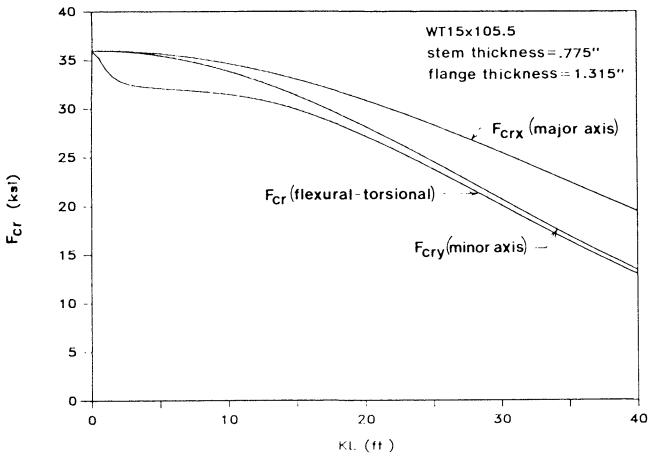

Fig. 9a. Effect of local slenderness on flexural-torsional buckling (axis of symmetry is minor axis)

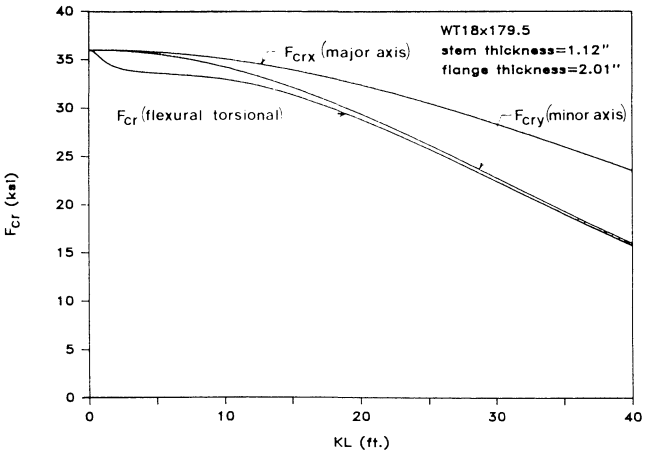

Fig. 9b. Effect of local slenderness on flexural-torsional buckling (axis of symmetry is minor axis)

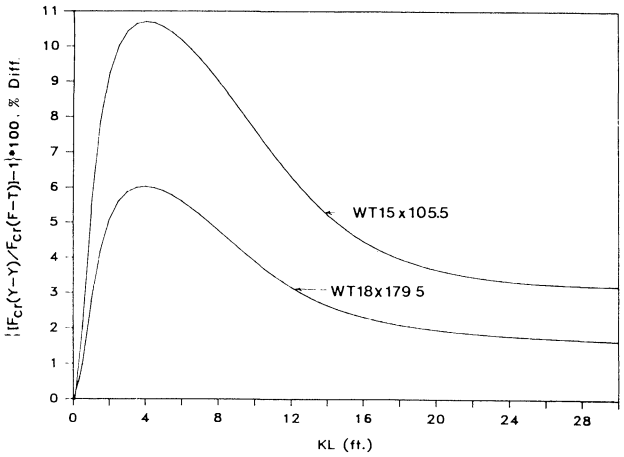

Fig. 10. Percent difference between F-T and Y-Y critical stress

strength calculation for W-shapes with a low a, such as the W12×336. However, since EC_w is an important parameter for most W-shapes, it should be combined with GJ in the more accurate column torsional strength evaluation, similar to the new LRFD beam lateral-torsional buckling limit state.

It can be concluded that torsional buckling is not ordinarily important for the design of W-shapes columns, provided adequate bracing against twist is furnished. However, if the section has a greater unbraced length for torsional buckling than for the minor (Y-direction) bending, torsional buckling may govern. For example, a W20×33 is braced every 10 ft in the Y-direction, every 20 ft in the X-direction, and has an unbraced length for torsional buckling of 20 ft. Referring to Fig. 14, this bracing arrangement results in torsional buckling being the governing limit state (see Appendix). Therefore, even though torsional buckling appears to be relatively insignificant for W-shapes, it may govern the strength if adequate torsional bracing is not provided.[12] In many cases, X or Y direction lateral bracing by rolled structural members provides sufficient strength and stiffness to also act as a torsional brace. A clear exception is rod bracing attached at a single localized point which does not effectively restrain twist.

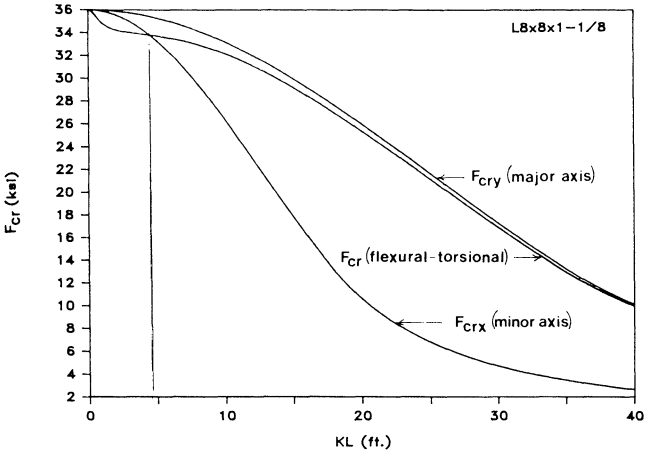

Fig. 11a. Critical stress for L8 × 1⅛ (axis of symmetry is major axis

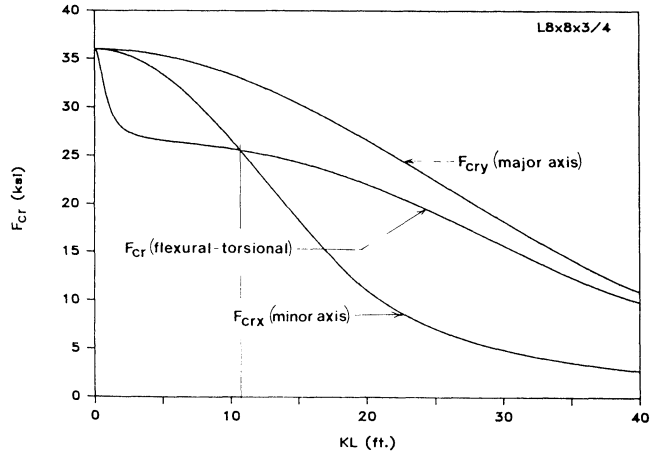

Fig. 11b. Critical stress for L8 × 8⅛ (axis of symmetry is major axis)

DESIGN AIDS

As the previous discussion elaborated, the LRFD Appendix E and ASD flexural-torsional buckling criteria add an additional dimension of complexity to the column design process. Fortunately, computer-aided design relieves most of the burden of the extra required calculations, but for spot checking and selected "long-hand" design, the LRFD Manual column load tables and graphical aids can be quite useful.

All the LRFD Manual column load tables for ϕP_{cr} can be directly used with factored loads without any modifications, since these design strengths automatically include any flexural-torsional buckling, local buckling, or interconnector spacing reductions. The latter is only applicable to built-up sections (such as double angles), but the former two limit states are relevant to both double angles and tees. Since the axial capacities of other common singly symmetric shapes—channels and equal leg angles—are not shown in this Manual, a simple graph has been developed to expedite the solution of the laborious Appendix E equation for F_e (Eq. A-E3-6). Figure 18 is valid for all singly symmetric compression members and represents the percent decrease in the critical elastic buckling stress due to flexural-torsional coupling from the smaller of F_{ey} or F_{ez}. At the limit of $H = 1$ for a

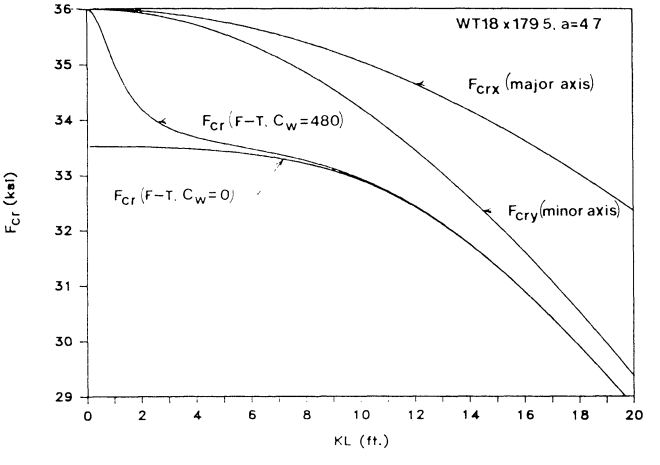

Fig. 12. C_w effect on critical stress for WT shape

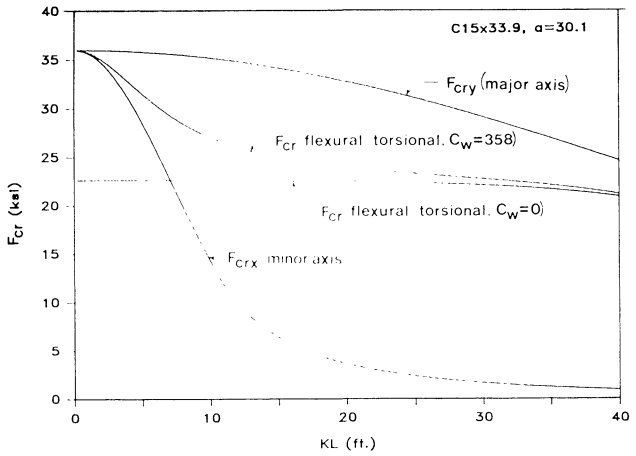

Fig. 13. C_w effect on critical stress for C shapes

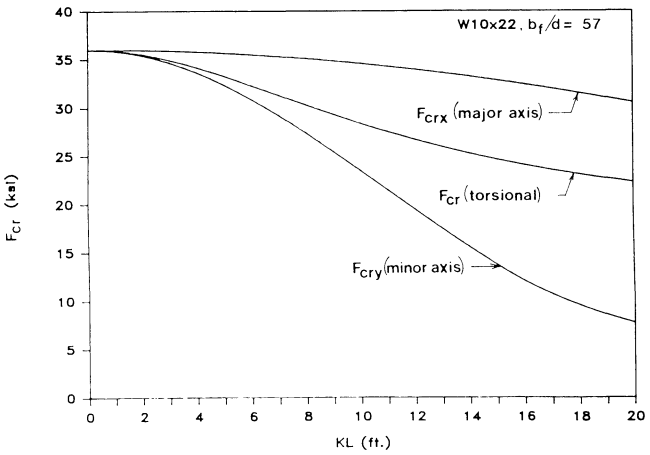

Fig. 14. Critical stress for W10 × 22

doubly symmetric shape, F_e is merely the smaller of F_{ey} or F_{ez} as discussed previously. Of course, the X-direction strength must also be checked. The independent variables are simply the $(F_2/F_1) > 1.0$ ratio and the H property of the shape. The maximum reduction occurs near $(F_2/F_1) = 1$ and low H. Conversely, as H increases or (F_2/F_1) becomes larger, the reduction becomes smaller, approaching the doubly symmetric $H = 1$ case at the limit. The following easy steps can be used with Fig. 18 in flexural-torsional buckling design/analysis:

1. Compute F_{ey} and F_{ez}
2. Set $F_1 = \min(F_{ey}, F_{ez})$
   $F_2 = \max(F_{ey}, F_{ez})$
3. Determine H, (F_1/F_2)
4. Read (F_e/F_1) from Fig. 18
5. Compute λ_e (LRFD) or $\left(\frac{Kl}{r}\right)_e$ (ASD)
6. Use column design curve to determine governing ϕP_{cr}
   $= \phi F_{cr} A$ (LRFD) or F_a (ASD) (flexural-torsional or S)

As an illustration, assume $P_u = 1{,}000$ kip for a truss compression chord WT18 × 150 (Y axis of symmetry is also the minor axis), A36, $KL_x = KL_y = 10$ ft.

A. Use LRFD Manual tables (pg. 2-79)
   $\phi P_{nx} = 1{,}310$ kip
   $\phi P_{cr} = \phi P_{ny} = 1{,}200$ kip (includes flexural-torsional effects)
   $1{,}000 < 1{,}200$ OK

B. Use Fig. 18
   1. $F_{ey} = 292$ ksi at $\left(\frac{Kl}{r}\right)_y = 31.3$
      $C_w = 278$ in.^{6}, $J = 32$ in.^{4}, $\bar{r}_o = 7.30$ in.
      $F_{ez} = 150$ ksi by Eq. (A-E3-12)

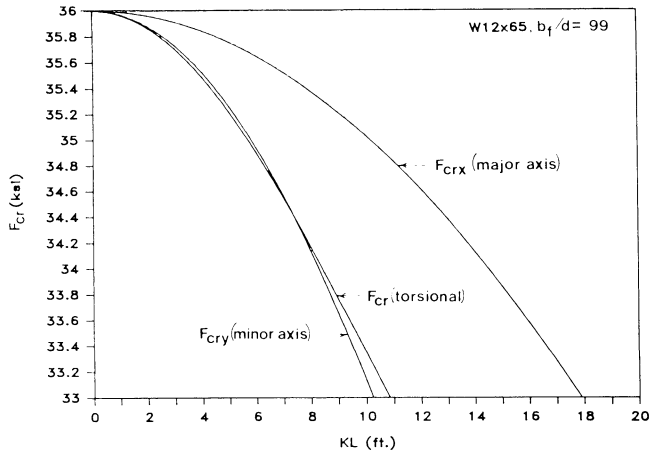

Fig. 15. Critical stress for W12 × 65

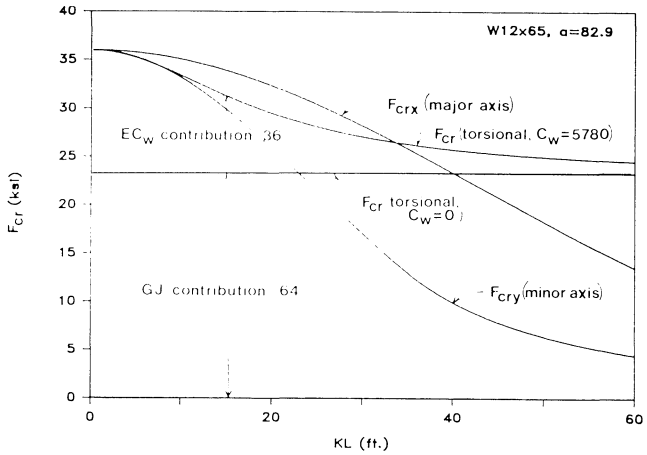

Fig. 16. C_w effect on compressive strength of W12 × 65

2. $F_1 = 150$; $F_2 = 292$
3. $H = 0.797$; $(f_2/F_1) = 1.95$
4. (F_e/F_1) 3 0.85
   $F_e \approx 127.5$
5. $\lambda_e = \sqrt{\frac{36}{127.5}} = 0.531$
6. $\phi F_{cr} = 27.2$ ksi
   $\phi P_{cr} = 27.2\ (44.1) = 1{,}200$ kip O.K.

Note: *without* flexural-torsional effects:

$\phi P_{cr} = \phi P_{ny} = \phi F_{cry} A = 29.05\ (44.1) = 1{,}281$ kip, or about 6.8% higher than 1,200 kip

It can be shown[6] that for singly symmetric single angle columns, $H = 0.625$ and flexural-torsional buckling will govern only when the minor principal axis

$$\left(\frac{Kl}{r}\right)_x^{\max} < 5.4\left(\frac{b}{t}\right)$$

The limiting slenderness (b/t) for angle legs to prevent local buckling is $76/\sqrt{F_y}$, as in ASD. For A36 steel angles that satisfy this local slenderness criterion, simple flexural buckling will always govern above a maximum member slenderness of 68.4, again demonstrating that for this case, flexural-torsional buckling effects will become evident only for shorter unbraced lengths. For stockier legs and smaller (b/t)s, this transition limit will correspondingly decrease. For example, in Fig. 11(a) for a L8 × 8 × 1⅛, flexural-torsional buckling F_e is less than F_{ex} in the graph for KL less than appoximately 5 ft., which for minimum $r_x = 1.56$ in. translates into $(Kl/r)_x = 38.5$. The local slenderness $(b/t) = 7.11$ results in $(Kl/r)_x = 5.4 \times 7.11 = 38.4$, as predicted.

Similar to equal leg angles, channels' Y-axis of symmetry is also the major principal axis. Therefore, flexural-torsional buckling will only control below a certain unbraced length. Figure 19 from the AISI Cold-Formed Design Manual provides a convenient graphical solution for this transition length. Hot-rolled channels have no lips and, thus, $c/a = 0$, b/a corresponds to b_f/d, and the t/a_2 can be approximated by $(t_w + t_f)/2d_2^2$, using an average of the flange and web thicknesses. Given a channel shape and its characteristic B_f/d and $(t_w + t_f)/2d^2$ this design aid can be used very easily. For example, for a C8 × 18.75, $b/a = .316$, $t/a^2 = .00686$, the transition unbraced length is about 20 in., meaning that simple flexural buckling will usually always govern.

It can be seen from Fig. 19 that flexural-torsional buckling for rolled channels will be inconsequential for all practical purposes at $(b_f/d) < 0.3$. For other channel shapes, the transition length can be estimated from this graph and the governing compression strength obtained with the help of Fig. 18.

A few more examples of LRFD compression members are provided in the Appendix.

CONCLUSIONS

An additional compression member strength limit state has been introduced in LRFD and the updated 1989 ASD. This flexural-torsional or torsional buckling will generally not govern for the stockier hot-rolled shapes that are at least singly symmetric and have governing effective lengths of about 10 ft. or more. Therefore, only relatively infrequent and remote cases will be encountered in practice wherein this new limit state can be important. Nevertheless, compliance of all designs with the applicable building codes and specifications must be assured independently by the responsible structural engineer. To help with this task, the relevant elastic buckling theory has been reviewed, graphical design aids and examples presented.

It is expected that this article will stimulate a greater awareness of flexural-torsional buckling implications for steel design and remove the mystery of this additional limit state.

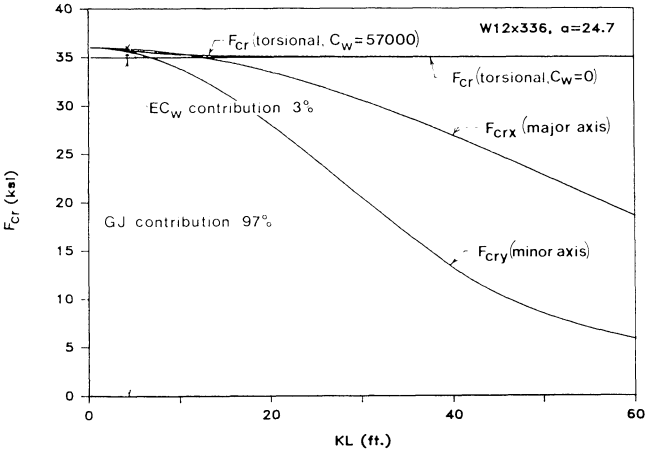

Fig. 17. C_w effect on compressive strength of W12 × 236

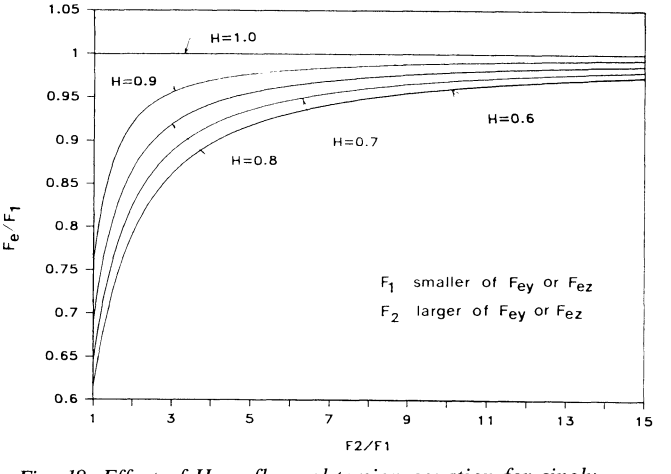

Fig. 18. Effect of H on flexural-torsion equation for singly symmetric shapes

REFERENCES

1. American Institute of Steel Construction, *Load and Resistance Factor Design Manual of Steel Construction,* lst ed., Chicago: AISC, 1986.
2. American Iron & Steel Institute, *Specification for the Design of Cold Formed Steel Structural Members,* August 19, 1986.
3. Zahn, Cynthia J., and Geerhard Haaijer, "Effect of Connector Spacing on Double Angle Compressive Strength," *Proceedings of the National Engineering Conference,* Chicago: AISC, 1987, pp. 25–3 through 25–21.
4. Brandt, G. D., "Flexural-Torsional Buckling for Pairs of Angles Used As Columns," AISC *Engineering Journal,* lst Quarter, 1988.
5. American Institute of Steel Construction, *Manual of Steel Construction,* 8th ed., Chicago: AISC, 1980.
6. Chajes, Alexander and George Winter, "Torsional-Flexural Buckling of Thin-Walled Members," ASCE *Structural Journal,* August 1965.
7. Yu, Wei-Wen, "Cold-Formed Steel Design," New York: Wiley-Interscience, 1985.
8. Chajes, Alexander, Pen J. Fang, and George Winter, "Torsional Flexural Buckling, Elastic and Inelastic, of Cold-Formed Thin Walled Columns," *Cornell Engineering Research Bulletin,* August 1966.
9. Bleich, Friedrich, *Buckling Strength of Metal Structures,* New York: McGraw-Hill Book Company, 1952.
10. Timoshenko, Stephen P. and James M. Gere, *Theory of Elastic Stability,* New York: McGraw-Hill Book Company, 1961, pp. 225–29.
11. American Institute of Steel Construction, *Torsional Analysis of Steel Members,* Chicago: AISC, 1983.

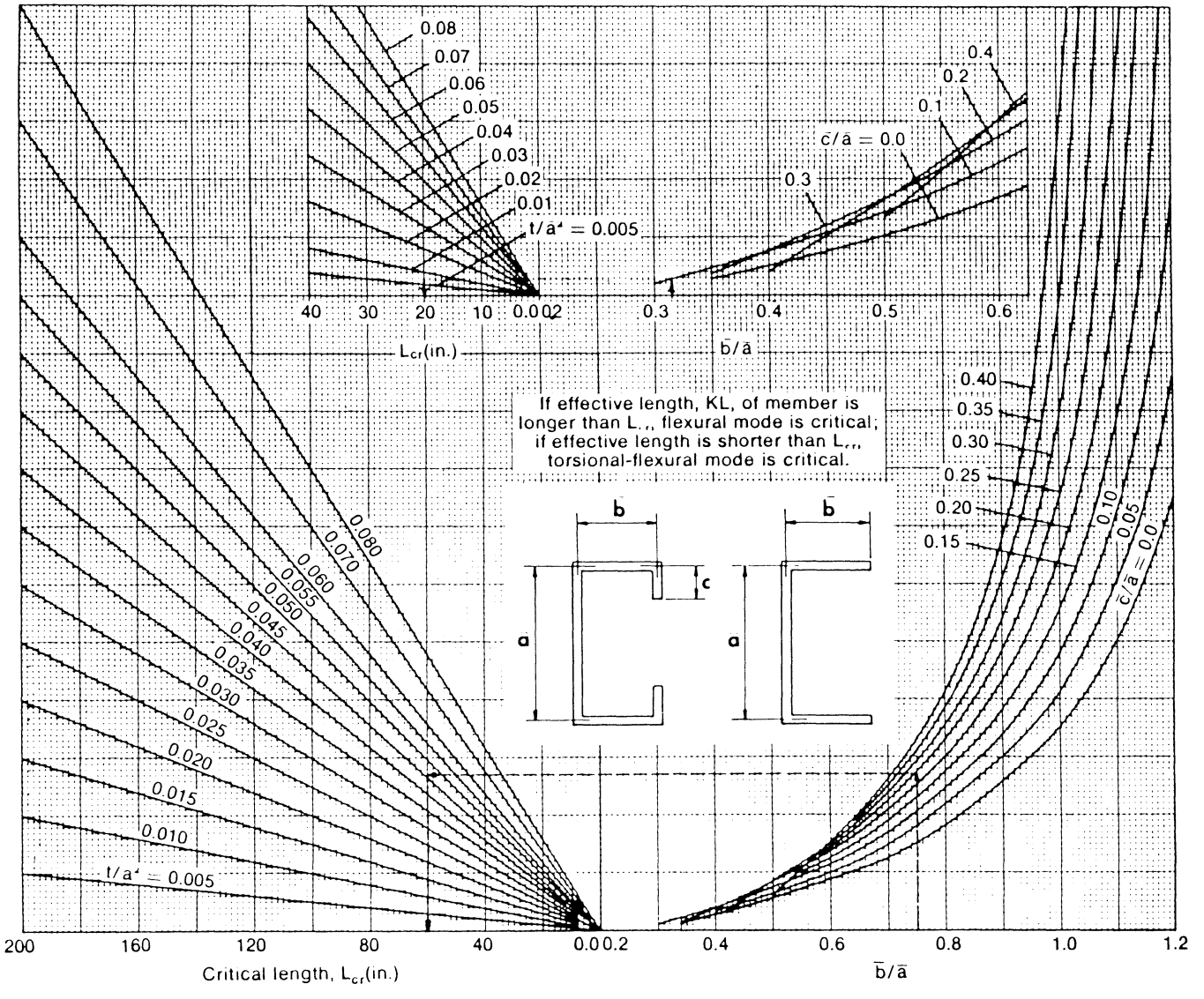

Figure 19

12. Brown, Jack H., "Bracing Requirements for Columns to Prevent Torsional Instability, Structural Engineering Practice, 2(4):1983–84.
13. American Institute of Steel Construction, *Specification for Structural Steel Buildings, Allowable Stress Design and Plastic Design,* Chicago: AISC, 1989.
14. American Institute of Steel Construction, *Specification for Allowable Stress Design of Single Angle Members,* Chicago: AISC, 1989.

NOMENCLATURE

A	Cross-sectional area, in.^{2}
A_g	Gross area, in.^{2}
C_w	Warping constant, in.^{6}
E	Modulus of elasticity of steel (29,000 ksi)
F_{cr}	Critical stress, ksi
F_a	Allowable compression stress, ksi
F_e	Elastic buckling stress, ksi
F_{ex}	Elastic flexural buckling stress about X-axis, ksi
F_{ey}	Elastic flexural buckling stress about Y-axis (axis of symmetry for singly symmetric shapes), ksi
F_y	Specified minimum yield stress of type of steel being used, ksi
F_1	Smaller of F_{ey} or F_{ez}, ksi
F_2	Larger of F_{ey} or F_{ez}, ksi
G	Shear modulus of elasticity of steel (11,200 ksi)
H	Flexural constant $= 1 - \left(\frac{x_o^{\,1} + y_o^{\,2}}{\bar{r}_o^{\,2}}\right)$
I_x, I_y	Moment of inertia about principal X and Y axes, respectively, in.^{4}
J	Torsional constant, in.^{4}
K_x, K_y, K_z	Effective length factor for X-axis, Y-axis, and torsional buckling, respectively
$\left(\frac{Kl}{r}\right)_e$	Equivalent slenderness ratio used in Allowable Stress Design
L	Unbraced length, in.
P_n	Nominal compressive axial strength, kips
Q	Full reduction factor for slender compression elements
r_x, r_y	Radius of gyration about principal X and Y axes, respectively, in.
$\bar{r}_o$	Polar radius of gyration about principal X and Y axes, respectively, in.
x_o, y_o	Coordinates of the shear center with respect to the centroid, in.
λ_e	Equivalent slenderness parameter
ϕ_c	Resistance factor for compression = 0.85

APPENDIX

Selected LRFD Design Examples

1. Assuming a centrally loaded, single angle, 6×6×½, A36, what is the controlling LRFD compression strength for

a) $KL_x = KL_y = KL_z = 10$ ft

b) $KL_x = KL_y = KL_z = 5$ ft

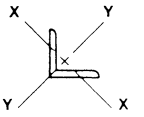

Alt. A—first check Eq. 3

a) $\left(\frac{Kl}{r}\right)_x^{max} = 5.4\left(\frac{b}{t}\right) = 5.2\ (12) = 64.8$

$r_x = 1.18$ in.; $\left(\frac{Kl}{r}\right)_x = \frac{10\times12}{1.18} = 101.7$

$101.7 > 64.8$, thus, simple minor axis flexural buckling controls

$\phi F_{crx} = 17.75$ ksi

$\phi P_{cr} = \phi F_{crx} A = 17.85\ (5.75) = 102.1$ kips

b) $\left(\frac{Kl}{r}\right)_x = \frac{5\times12}{1.18} = 50.8 \quad (\phi F_{crx} = 26.7 \text{ ksi})$

$50.8 < 64.8$, thus, flexural-torsional buckling controls

$$2\ (1.86)^2 = 1.18^2 + r_y^2$$

$r_y = 2.35$ in.

$\left(\frac{Kl}{r}\right)_y = \frac{5\times12}{2.35} = 25.53$

$F_{ey} = 439$ ksi

$J = 0.5$, $\bar{r}_o = 3.32$ in., $C_w = 1.32$

$H = 0.627$

$F_{ez} = 90.19$ ksi by Eq. A-E3-12

use Fig. 18: $F_2 = 441$

$$(F_2/F_1) = 5$$

read $(F_e/F_1) \approx 0.91$

$$F_e = 80.4 \text{ ksi}$$

$$\lambda_e = \sqrt{\frac{36}{80.4}} = 0.67$$

$\phi F_{cr} = 25.34$ ksi

$\phi P_{cr} = 25.34\ (5.75) = 146$ kips

Note: *without* flexural-torsional effects:

$$\phi P_{cr} = \phi F_{crx} A = 26.7\ (5.75) = 153.5 \text{ kips}$$

about 5.4% higher than 146 kips

Alt. B—directly compare flexural and flexural-torsional strengths

a) $\left(\frac{Kl}{r}\right)_x = 101.2$, thus $\phi F_{crx} = 17.85$ ksi

$\left(\frac{Kl}{r}\right)_y = \frac{10\times12}{2.35} = 51$

$F_{ey} = 110$ ksi

$F_{ez} = 88.36$ by Eq. A-E3-12

use Fig. 18: $F_1 = 88.4$; $F_2 = 110$

$(F_2/F_1) = 1.24$ and $H = 0.627$

read $(F_e/F_1) = 0.67$

$F_e = 59.2$

$$\lambda_e = \sqrt{\frac{36}{59.2}} = 0.78$$

$\phi F_{cr} = 23.7$ ksi

17.85 < 23.7, thus X flexural buckling controls

$\phi P_{cr} = 17.85\ (5.75) = 102.6$ kips

b) as before $F_{ey} = 441$ ksi

$F_{ez} = 88.36$

use Eq. A-E3-6 directly:

$$F_e = \frac{441+88.4}{2(.627)}\left[1 - \sqrt{1 - \frac{4(441)(88.4)(.627)}{(441+88.4)^2}}\right]$$

$F_e = 422[1-\sqrt{1-0.349}] = 81.5$ ksi

(81.5 compares well to 80.4 determined previously by Fig. 18)

as before, $\phi P_{cr} = 146$ kips

2. For a central compression factored load of P_u =75 kips,

$KL_x = KL_y = KL_z = 10$ ft, select minimum weight

A 36 channel section

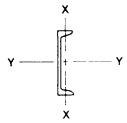

estimate $\left(\frac{Kl}{r}\right)_y \approx 120$, then $\phi F_{cr} = 14.3$ ksi

$$A_{min} = \frac{75}{14.3} = 5.25 \text{ in.}^2$$

try C12×30

$A = 8.82$ in.^{2}
$b_f = 3.17$ in.
$d = 12$ in.
$r_y = 4.29$ in.
$r_x = 0.763$ in.
$J = 0.87$ in.^{4}
$C_w = 151$ in.^{6}
$\bar{r}_o = 4.55$ in.
$H = 0.919$

$$\left(\frac{Kl}{r}\right)_x = \frac{10\times12}{0.763} = 157.3$$

$\phi F_{crx} = 8.6$ ski

$\phi P_{cr} = 8.7\ (8.82) = 75.9$ k > 75k **ok**

$\frac{b_f}{d} = \frac{3.17}{12} = 0.26$, from Fig. 19, since

$KL = 10$ ft (40 in., only simple flexural buckling will govern design

or check Fig. 18

$\left(\frac{Kl}{r}\right)_y = \frac{120}{4.29} = 28$; $F_{ey} = 365$ ksi,
$F_{ez} = 70$ ksi by Eq. A-E3-12

$(F_2/F_1) = 5.2$
$(F_e/F_1) = 0.97$
$F_e = 67.9$

$$\lambda_e = \sqrt{\frac{36}{67.9}} = 0.73$$

$\phi F_{cr} = 24.5$ ksi > 8.7 ksi **ok**
minor axis controls

3. A W10×22, A36 column has $(KL)_y = 10$ ft and $(KL_x) = (KL)_z = 20$ ft. What is its design strength?

$A = 6.49$ in.^{2}
$r_x = 4.27$ in.
$r_y = 1.33$ in.
$J = 0.24$ in.^{4}
$C_w = 275$ in.^{6}

minor axis: $\left(\frac{Kl}{r}\right)_y = \frac{10\times12}{1.33} = 90.2$; $\phi F_{cry} = 19.9$ ksi

major axis $\left(\frac{Kl}{r}\right)_x = (\frac{20\times12}{4.27}) = 56.2 < \left(\frac{Kl}{r}\right)_y$

torsional buckling: $F_{ez} = 31.5$ by Eq. A-E3-12

$$\lambda_e = \sqrt{\frac{36}{31.5}} = 1.07$$

$\phi F_{cr} = 18.7$ ksi < 19.9 ksi

thus, torsional buckling controls

$\phi P_{cr} = 18.7\ (6.49) = 121$ kips